様　式　Ｃ－１９、Ｆ－１９－１、Ｚ－１９　（共通）

科学研究費助成事業　　研究成果報告書

令和　３ 年　 ６ 月 １７ 日現在

機関番号：１２６０８
研究種目：研究活動スタート支援
研究期間：2019～2020
課題番号：１９Ｋ２３７２１

研究課題名（和文）Atomistic mechanism of the oligomerization of p53 protein in DNA scanning

研究課題名（英文）Atomistic mechanism of the oligomerization of p53 protein in DNA scanning

研究代表者
ＴＲＡＮ　ＰＨＵＯＣ・ＤＵＹ（TRAN, PHUOC DUY）

東京工業大学・生命理工学院・助教

研究者番号：５０８４８５４６

交付決定額（研究期間全体）：（直接経費）　　2,200,000円

研究成果の概要（和文）：我々は、タンパク質の天然変性領域（IDR）と標的タンパク質との結合および解離の経路を調べる方法を開発し、この方法をp53標的に適用した。その結果、IDRはまず正しい結合ポケットを見つけるために構造選択を行い、次に正しいネイティブな結合構造に入るために誘導されたフィッティングメカニズムを行うという複数の状態を経て、結合・解離経路の詳細な原子メカニズムを発見しました。最終的には、結合界面の脱水と二次構造の形成が、ネイティブな結合構造の形成に大きく貢献します。さらに、今回開発した手法は、実験データと一致した滞留時間の推定が可能です。

研究成果の学術的意義や社会的意義
This research results provide detailed atomic structures of TAD-p53 bound to MDM2 which can potentially treat as drug target to help to prevent the p53 related diseases such as cancer and neurodegenerative diseases.

研究成果の概要（英文）：We developed the method to investigate the association and dissociation pathway of intrinsically disordered region of protein (IDR) to the targeted protein, and apply this method to p53 target. We find the detailed atomic mechanism of association and dissociation pathway through multiple states in which the IDR first perform the conformational selection to find the correct binding pocket following by the induced fitting mechanism to enter the correct native bound conformation. In the final state, the dehydration of the binding interfaces and secondary structure formation greatly contribute to the formation of the native bound structure. In addition, our recently developed method has ability to estimate the residence time in agreement with experimental data.

研究分野：生物物理

キーワード：a/dPaCS-MD　p53　IDP　docking　koff

１．研究開始当初の背景

p53 is a 53 kDa extremely flexible protein, composed of N terminal transactivation domain (NTD) connecting to DNA-binding domain (DBD) via a proline-rich region (PRR) and being linked with tetramerization domain (TED) and C-terminal domain (CTD). NTD and CTD are found to be intrinsically disordered. p53 involves in such broad range of biological processes such as translation, proliferation, autophagy, cellular response, etc. by directly or indirectly interacting with a variety of the other biomolecules. Homo-tetramer of p53 has been found increasing the DNA binding affinity up to 100 times comparing to the p53 monomer. Heterodimer with MDM2 inhibits the tumor suppressor function. Moreover, heterodimer with E6 protein of HPV virus or SV40 protein triggers the cancer. Recently, p53 has been found that it even interacts with mRNA to trigger the transcription. Therefore, understanding the association (AS) and dissociation (DS) process of p53 at molecular level is crucial step within “long-term war” to eliminate the century-disease Cancer. Although recently more partial structures of p53 have been solved by experiments, flexibility of p53 prevents the effort to fully understand the AS, DS at atomistic level experimentally. Recent advances of molecular dynamics (MD) simulations can allow the full consciousness.

２．研究の目的

In this research, we focus on the understanding of the association/dissociation mechanism of intrinsically disordered region of proteins (IDR) which is mainly driving the activity of p53 protein. We focus to solve the following problem:

1. Reconstructing the association/dissociation pathway of N terminal domain of p53 to MDM2 protein.
2. Establish the efficient method to estimate the binding affinity and residence time which is desirable for drug design.

３．研究の方法

In this research, we develop the new simulations method to estimate the kinetic rates and the native bound conformations of the given complex using the new simulation algorithm so-called a/dPaCS-MD together with Markov State Modeling as shown in Figure 1.

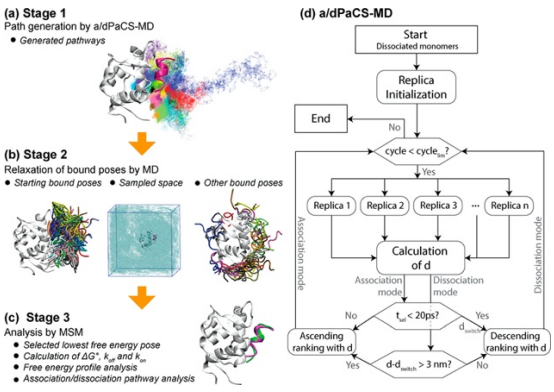

Figure 1. The a/d PaCS-MD algorithm. a, b, c plots show the visualization of each stage in the procedure. d) shows the a/dPaCS-MD algorithm.

In stage 1, we initially started PaCS-MD in the association mode from a completely dissociated state. PaCS-MD switches to the dissociation mode if the top-ranked snapshot is

selected in the first 20 ps (τ_{select} < 20 ps) of the 0.1 ns MD trajectories, at which the approaching speed significantly slows or gets stuck. The choice of τ_{select} < 20 ps was decided based on the results of our previous work, in which snapshots in the bound state were mostly selected from the initial 20 ps of the trajectories. In the dissociation mode, if d increases more than 3 nm from the previous switching point, PaCS-MD again switches to the association mode. When IDR peptide made contact with target protein in the top-ranked snapshot in each cycle, the structure was stored as a bound pose. All the selected bound poses are carried out classical MD simulations to optimize the conformations. In stage 3, all the data from stage 1 and 2 are used to construct the Markov State Model.

４．研究成果

We applied the a/dPaCS-MD to the MDM2 and TAD-p53 system. The prefix "p" before residue index denotes that residue belongs to TAD-p53 while "m" denotes for belonging to MDM2.

1. Mechanism of association pathway of TAD-p53 to MDM2

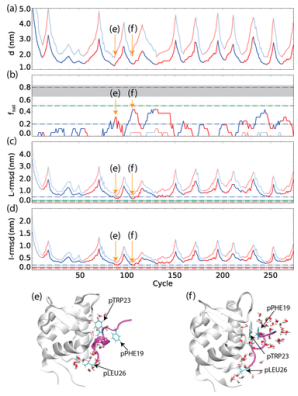

Figure 2. Evolution of parameters and structures in stage 1. (a) The inter-COM distance d, (b) the fraction of native contacts (fnat), (c) the ligand (L-), and (d) interface root-mean-square deviations (I-rmsd's). (e,f) Representative structures at (e) cycle 89 and (f) cycle 107 indicated by arrows in (a)–(d) are shown. Blue and red solid lines in (a)–(d) denote the association and dissociation modes, respectively. The thinner and thicker lines show the maximum and minimum at each cycle. Gray shaded areas show the range of standard deviations during the 1 μs MD simulation starting with the crystal complex structure. Red, green, and blue horizontal lines show the ranges of high, medium, and acceptable qualities in CAPRI. In (e) and (f), the key residues pPHE19, pTRP23, and pLEU26 are shown as cyan stick models. Water molecules bound to TAD-p53 are also shown.

The L- and I-rmsd's were highly correlated, and f_{nat} was anticorrelated with d, respectively. After several association events, TAD-p53 adopted conformations similar to the crystal complex structure. After several association events, TAD-p53 adopted conformations similar to the crystal complex structure. Snapshots of cycles 89 and 107, whose structures are shown in Figure 2e and f, achieved the lowest L-rmsd of 0.36 and 0.34 nm, the lowest I-rmsd of 0.20 and 0.19 nm, and the highest fnat of 0.31 and 0.44, respectively. In the structures at around cycles 128–132 and 244, fnat also reached 0.44, but I-rmsd was slightly higher than in the former cases, and L-rmsd reached the range of acceptable quality in CAPRI. The best snapshots (cycles 89 and 107) adopted relatively helical structures. We noticed many water-mediated contacts between MDM2 and TAD-p53, but the binding interface should be more dehydrated to achieve the complete binding. In addition, Figure 2e shows that, at cycle 89, pPHE19 pointed toward the opposite side of the binding interface, and TAD-p53 had fewer water-mediated contacts as compared to those at cycle 107 (Figure 2f), while the hydrophobic interactions with MDM2 were better formed at cycle 107. These results show that TAD-p53 found reasonable binding poses in stage 1 without using any guiding force.

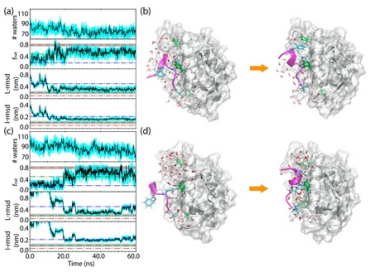

Figure 3. Examples of the dehydration/structure relaxation process starting from transiently bound poses to the lowest free energy poses in stage 2. (a,b) The lowest and (c,d) the second lowest free energy microstates. (a,c) Time evolution of the number of water molecules around TAD-p53, fraction of native contacts (fnat), and ligand (L-) and interface rmsd's (I-rmsd's). Cyan thin lines show actual instantaneous values, and black thick lines show smoothed averaged values. The meaning of the gray shaded areas, and the horizontal red, green, and blue lines, are the same as in Figure 3b–d. (b,d) The initial (left) and final (right) MD structures.

In the beginning of trajectory to native bound state, TAD-p53 did not take a helical form, and its N-terminal side including pPHE19 protruded into the solvent. Upon helical formation of the central region of TAD-p53, pPHE19 moved between mTYR63 and pTRP23. At the same time, the complex interface was dehydrated, and π–π stackings of pPHE19, pTRP23, and mTYR63 were formed. In some of the best snapshots, f_{nat} reached the high-quality range in CAPRI, and L-rmsd reached in the medium range. In contrast, Figure 3c,d show a typical case in which the initial structure (a snapshot from cycle 88) had almost no native contacts, but all of the quantities improved after 10 ns, reaching the high-quality range in f_{nat}, and the other quantities almost reached the acceptable range. Even in the case in which MD simulation was started from the crystal structure, the complex structure was judged to be in the medium range using the CAPRI criteria. Overall, we conclude that MD in stage 2 successfully optimized the decoy structures in some cases, including structures very similar to the crystal structure. In both cases shown in Figure 3, dehydration of the complex interface as well as final relaxation and fitting of the interface side chains occurred during this stage. TAD-p53 cannot relax to the lowest free energy state without dehydration, indicating that hydration is the key for completing complex formation.

2. Efficient method to estimate the kinetic rates

We chose 3000 clusters and a lag time of 50 ps as the optimum parameters. We conducted the volume correction to obtain ΔG° using the estimated sampling concentration of 0.041 M. The final kinetic rates and standard binding free energy are in agreement with the range of reported experimental values, indicating that this procedure can accurately predict binding affinity and kinetic rates. Although k_{on} is still in the range of the experimental values, it is smaller than values obtained in our previous work, probably due to the current broader conformational sampling, including non-native binding poses, which slows the association process.

The global minimum of the free energy landscape showed a free energy value of −11.4 kcal/mol relative to the highest energy state set to 0. The corresponding structure at the global minima (f_{nat} = 0.94 ± 0.02, L-rmsd = 0.17 ± 0.04 nm, and I-rmsd = 0.19 ± 0.01 nm) is very similar to the crystal complex structure. Therefore, the current procedure can select a native-like complex structure as the structure with the lowest free energy, indicating that this method can be used as a flexible docking procedure.

The free energy landscape of MDM2/TAD-p53 association/dissociation was mapped onto the first two time-independent components (TICs 1 and 2) and is shown in Figure 4a. Five MDM2-bound intermediates whose free energies were lower than or equal to −10.0 kcal/mol were identified (Figure 4a) and were rank-ordered from the lowest free energy as CI1–CI5. As will be shown later, CI2 is the dominant intermediate on the path toward CN. In CI1, TAD-p53 formed a relatively extended structure, and its orientation was very different from that of CN. In this case, pASP21 formed a salt bridge with mHIS52, and pPHE19 and pTRP23 formed hydrophobic contacts with MDM2, which probably led to the lowest binding free energy among the CIs but an incorrect hydrophobic core. In CI2, TAD-p53 adopted a structure without regular main-chain hydrogen bonds, and the key hydrophobic residues, pPHE19 and pTRP23, did not make good contacts with MDM2, similar to the structures shown on the left of Figure 2b,d due to the presence of many water molecules at the complex interface. We noticed that, in CI2, pLEU26 contacted mILE50, resulting in initial hydrophobic interactions on the path toward CN. The free energy of CI2 is ~2 kcal/mol higher than that of MN in the monomeric state. CI2 is structurally similar to unbound state of TAD-p53 whose free energy is ~1 kcal/mol higher than that of global minimum of free state TAD-p53. The C_α-rmsd between CI2 and MI3 is 0.28 nm. In CI3, pPHE19 and pTRP23 pointed more to MDM2. In addition, the interface of CI3 was more dehydrated as compared to that of CI2, but TAD-p53 was more extended. TAD-p53 in CI4 mostly formed an α-helix but was bound to the bottom of the binding site. This complex was stabilized by a non-native aromatic cluster formed by pPHE19, pTRP23, and mTYR96. TAD-p53 in CI5 bound to MDM2 with an extended structure and upside down. In this case, pPHE19 contacted MDM2, pTRP23 nearly made CH-π interactions with mTYR51, and pLEU26 formed hydrophobic interactions with mILE50. Our free energy landscape shows similarity with the predicted kinetic maps of MDM2 complexed with PMI peptide.

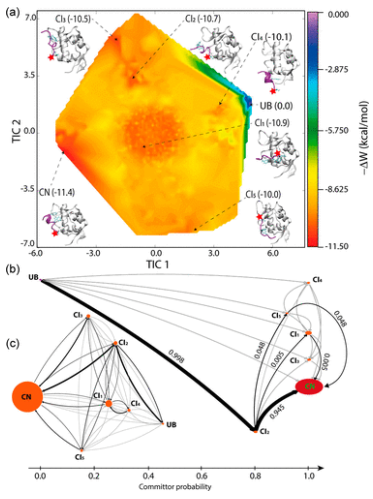

Figure 4. Association/dissociation process of the MDM2/TAD-p53 complex. (a) Free energy landscape of the complex projected onto the space spanned by the first two TICs. Representative structures of seven macrostates and their positions are shown. UB (unbound), CI1–CI5 (complex intermediates rank ordered from the lowest free energy), and CN (complex native). The key residues pPHE19, pTRP23, and pLEU26 are shown as stick models. The red "★" on the TAD-p53 structures denote the C-terminus. (b) Fraction of the flux of TAD-p53 association to MDM2 calculated from a coarse-grained MSM with seven macrostates. Relative positions of the macrostates along the abscissa show committor probabilities. The value near each arrow shows the fraction of the flux. Pathways with high fractions are shown by black lines. (c) Visualization of the transition matrix among the macrostates. The line thickness is proportional to the probability, and the major pathways are shown in black.

５．主な発表論文等

〔雑誌論文〕　計6件（うち査読付論文　3件／うち国際共著　6件／うちオープンアクセス　2件）

１．著者名 Tran Duy Phuoc、Kitao Akio	４．巻 16
２．論文標題 Kinetic Selection and Relaxation of the Intrinsically Disordered Region of a Protein upon Binding	５．発行年 2020年
３．雑誌名 Journal of Chemical Theory and Computation	６．最初と最後の頁 2835～2845
掲載論文のDOI（デジタルオブジェクト識別子） 10.1021/acs.jctc.9b01203	査読の有無 有
オープンアクセス オープンアクセスとしている（また、その予定である）	国際共著 該当する

１．著者名 Takaba Kenichiro、Tran Duy Phuoc、Kitao Akio	４．巻 152
２．論文標題 Edge expansion parallel cascade selection molecular dynamics simulation for investigating large-amplitude collective motions of proteins	５．発行年 2020年
３．雑誌名 The Journal of Chemical Physics	６．最初と最後の頁 225101～225101
掲載論文のDOI（デジタルオブジェクト識別子） 10.1063/5.0004654	査読の有無 無
オープンアクセス オープンアクセスではない、又はオープンアクセスが困難	国際共著 該当する

１．著者名 Huang Shuya Kate、Pandey Aditya、Tran Duy Phuoc、Villanueva Nicolas L.、Kitao Akio、Sunahara Roger K.、Sljoka Adnan、Prosser R. Scott	４．巻 184
２．論文標題 Delineating the conformational landscape of the adenosine A2A receptor during G protein coupling	５．発行年 2021年
３．雑誌名 Cell	６．最初と最後の頁 1884～1894.e14
掲載論文のDOI（デジタルオブジェクト識別子） 10.1016/j.cell.2021.02.041	査読の有無 無
オープンアクセス オープンアクセスではない、又はオープンアクセスが困難	国際共著 該当する

１．著者名 Tucs Andrejs、Tran Duy Phuoc、Yumoto Akiko、Ito Yoshihiro、Uzawa Takanori、Tsuda Koji	４．巻 5
２．論文標題 Generating Ampicillin-Level Antimicrobial Peptides with Activity-Aware Generative Adversarial Networks	５．発行年 2020年
３．雑誌名 ACS Omega	６．最初と最後の頁 22847～22851
掲載論文のDOI（デジタルオブジェクト識別子） 10.1021/acsomega.0c02088	査読の有無 無
オープンアクセス オープンアクセスではない、又はオープンアクセスが困難	国際共著 該当する

１．著者名 Duy Phuoc Tran, Hata Hiroaki, Ogawa Takumi, Taira Yuta, Kitao Akio	４．巻 22
２．論文標題 PaCS-MD/MSM : Parallel Cascade Selection Molecular Dynamic Simulation in Combination with Markov State Model as an Efficient non-Bias Sampling Method	５．発行年 2020年
３．雑誌名 アンサンブル : 分子シミュレーション研究会会誌	６．最初と最後の頁 151~156
掲載論文のDOI（デジタルオブジェクト識別子） なし	査読の有無 有
オープンアクセス オープンアクセスではない、又はオープンアクセスが困難	国際共著 該当する

１．著者名 Tran Duy Phuoc、Tada Seiichi、Yumoto Akiko、Kitao Akio、Ito Yoshihiro、Uzawa Takanori、Tsuda Koji	４．巻 11
２．論文標題 Using molecular dynamics simulations to prioritize and understand AI-generated cell penetrating peptides	５．発行年 2021年
３．雑誌名 Scientific Reports	６．最初と最後の頁 10630
掲載論文のDOI（デジタルオブジェクト識別子） 10.1038/s41598-021-90245-z	査読の有無 有
オープンアクセス オープンアクセスとしている（また、その予定である）	国際共著 該当する

〔学会発表〕　計5件（うち招待講演　3件／うち国際学会　5件）

１．発表者名 Tran Phuoc Duy, Akio Kitao
２．発表標題 Calculation of binding free energy and kinetic rates with flexible protein docking
３．学会等名 Annual Meeting of the Biophysical Society of Japan（招待講演）（国際学会）
４．発表年 2019年

１．発表者名 Duy Tran
２．発表標題 Biomolecular Functional Design: an Introduction to Recent Advances
３．学会等名 The 58th Annual Meeting of the Biophysical Society of Japan（招待講演）（国際学会）
４．発表年 2020年

１．発表者名
Yuta Taira, Duy Tran, Akio Kitao

２．発表標題
DNA binding mechanisms of the p53 C-terminal domain elucidated by MD simulation

３．学会等名
The 58th Annual Meeting of the Biophysical Society of Japan（国際学会）

４．発表年
2020年

１．発表者名
Yoshiki Miyazawa, Phuoc Duy Tran, Kazuhiro Takemura, Akio Kitao

２．発表標題
Kinetic rate evaluation for protein complexes by PaCS-MD/MSM

３．学会等名
The 58th Annual Meeting of the Biophysical Society of Japan（国際学会）

４．発表年
2020年

１．発表者名
Duy Tran, Akio Kitao

２．発表標題
When computer simulations meet machine learning: unveiling the dynamics of biomolecular complexes

３．学会等名
The 9th Tokyo Tech International Symposium on Life Science and Technology（招待講演）（国際学会）

４．発表年
2020年

〔図書〕　計0件

〔産業財産権〕

〔その他〕

―

６．研究組織

	氏名 （ローマ字氏名） （研究者番号）	所属研究機関・部局・職 （機関番号）	備考

７．科研費を使用して開催した国際研究集会

〔国際研究集会〕　計0件

８．本研究に関連して実施した国際共同研究の実施状況

共同研究相手国	相手方研究機関